

Supplementary Information

Endo180 and basement membrane stiffness induce OXPHOS and neoplasia in aging prostate epithelia

Lucia Pastro¹, Jennyfer Martínez², Santiago Fontenla¹, Ana C. Chiale¹, María P. Frade¹,
Andrea S. Díaz¹, Rodrigo Martino-Kunsch¹, Laura Castro², Lysann Schenk³, Celia Quijano²,
Justin Sturge⁴, Mercedes Rodríguez-Teja^{1*}

¹Departamento de Genética, Facultad de Medicina, Universidad de la República; 11800 Montevideo, Uruguay.

²Departamento de Bioquímica, Facultad de Medicina and Centro de Investigaciones Biomédicas (CEINBIO), Universidad de la República; 11800 Montevideo, Uruguay.

³Institute of Biotechnology, Faculty Environment and Natural Sciences, Brandenburg University of Technology Cottbus-Senftenberg; 01968 Senftenberg, Germany.

⁴Centre for Biomedicine, Hull York Medical School, Faculty of Health Sciences, University of Hull; United Kingdom.

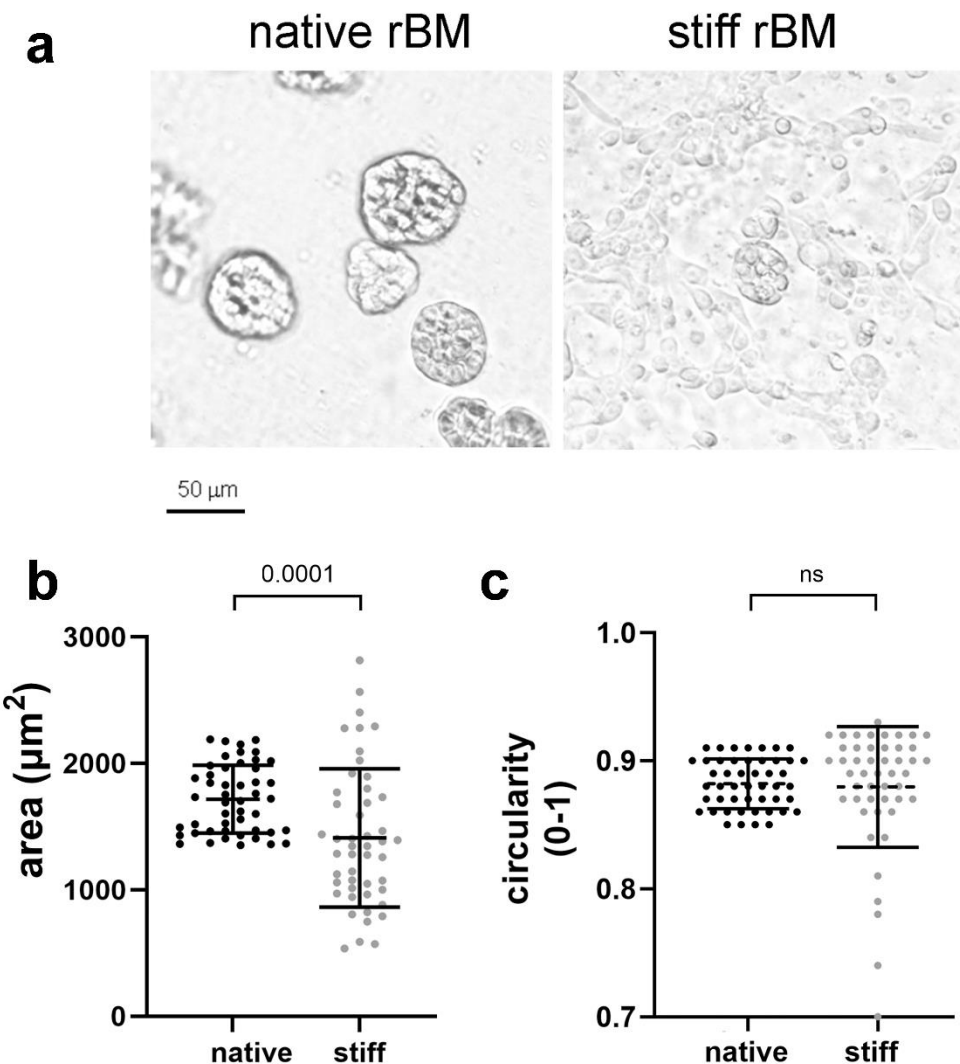
*Corresponding author: mercedesrodriguez@fmed.edu.uy

Table of contents:

Supplementary figure 1. Prostate epithelial acini morphology in stiff basement membrane	p3
Supplementary table 1. Mapping of Illumina RNA-seq reads	p4
Supplementary table 2. Variants in genomic region surrounding PAM site in Endo180-KO cells	p4
Supplementary table 3. Mapping of Illumina RNA-seq reads in Ctrl-acini and Endo180-KO acini	p5
Supplementary figure 2. OXPHOS genes upregulated by basement membrane stiffness are common to wild-type and control prostate epithelia	p6
Supplementary figure 3. Downregulation of cytoskeletal motor activity, receptor-signaling, tissue development, exosomes and cornified envelope in Endo180-KO prostate epithelia	p7
Supplementary figure 4. Gene ontology terms upregulated by basement membrane stiffness in control and Endo180-KO prostate epithelia	p8
Supplementary figure 5. Endo180 and basement membrane stiffness cooperate to sustain the hallmarks of cancer in prostate epithelia	p9
Supplementary figure 6. CD147 and OXPHOS genes remain positively correlated in Gleason score 6 and higher prostate cancer	p10
Supplementary figure 7. Endo180 but not CD147 is positively correlated with age at initial prostate cancer diagnosis	p12
Supplementary figure 8. Endo180 is an age-related time-bomb for metastatic prostate cancer	p13
Supplementary table 4. Oligonucleotide sequences used in this study	p15

Supplementary Data content (Excel files):

Supplementary data 1. DEGs in Wt-acini in stiff-BM versus native-BM
Supplementary data 2. GO terms in Wt-acini in stiff-BM versus native-BM
Supplementary data 3. DEGs in Ctrl-acini in stiff-BM versus native-BM
Supplementary data 4. DEGs in Endo180-KO-acini in stiff-BM versus native-BM
Supplementary data 5. DEGs in Wt/Ctrl intersect and KO only (stiff-BM versus native-BM)
Supplementary data 6. GO terms in Wt/Ctrl intersect and Endo180-KO only (stiff-BM versus native-BM)
Supplementary data 7. Upregulated terms in Ctrl-acini in stiff-BM versus native-BM
Supplementary data 8. GO terms in Endo180-KO-acini (stiff-BM versus native-BM)
Supplementary data 9. Repressed cancer hallmark gene enrichments linked to Endo180 expression in prostate acini in stiff-BM versus native-BM
Supplementary data 10. Sustained cancer hallmark gene enrichments linked to Endo180 expression in prostate acini in stiff versus native BM



Supplementary figure 1. Prostate epithelial acini morphology in stiff basement membrane. a) Bright field images of wild-type, wt, RWPE-1 cells grown for 6 days in native or stiff basement membrane (BM) (scale bar = 50 μ m). **b)** Cross sectional acinar area (mean \pm SD, μm^2) and **c)** circularity score (mean \pm SD, circular = 1, polygonal = 0); 48 acini analyzed; Mann-Whitney, two-tailed test, p value ≤ 0.05 , ns = not significant.

Supplementary Table 1. Mapping of Illumina RNA-seq reads

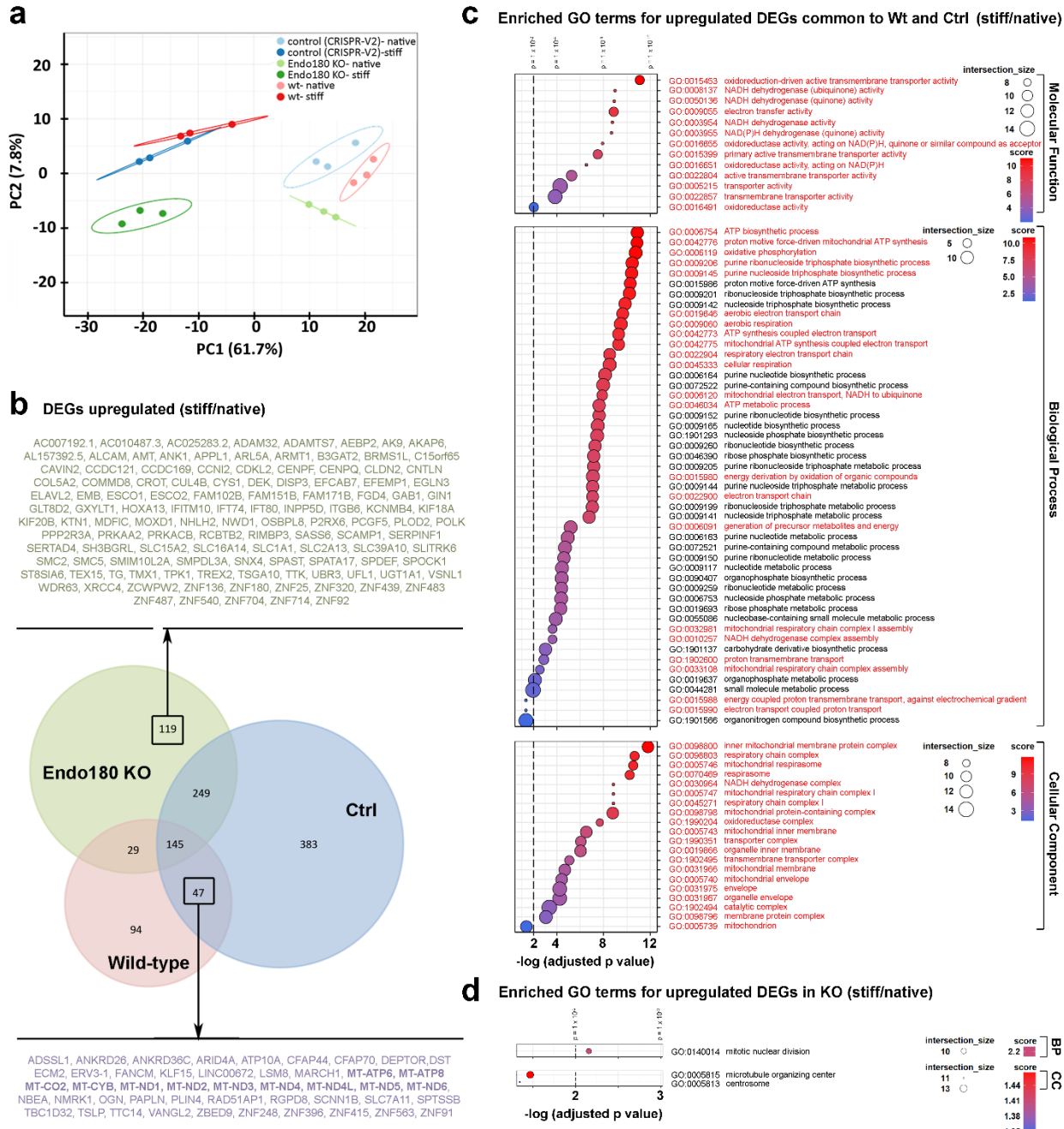
3D culture	Sample	Total reads	Total mapped reads (paired)*	% mapped
wild type acini native-BM	wt n1	22126486	14327897	64.75
	wt n2	25951344	15259917	58.80
	wt n3	23676542	16960460	71.63
wild type acini stiff-BM	wt s1	26241311	16190906	61.70
	wt s2	30244238	17744321	58.67
	wt s3	27141741	15783643	58.15
average % total mapped reads				62.29
* reads mapped to annotated genes				
BM, basement membrane; wt, wild type; n, native; s, stiff				

Supplementary Table 2. Variants in genomic region surrounding PAM site in Endo180-KO cells

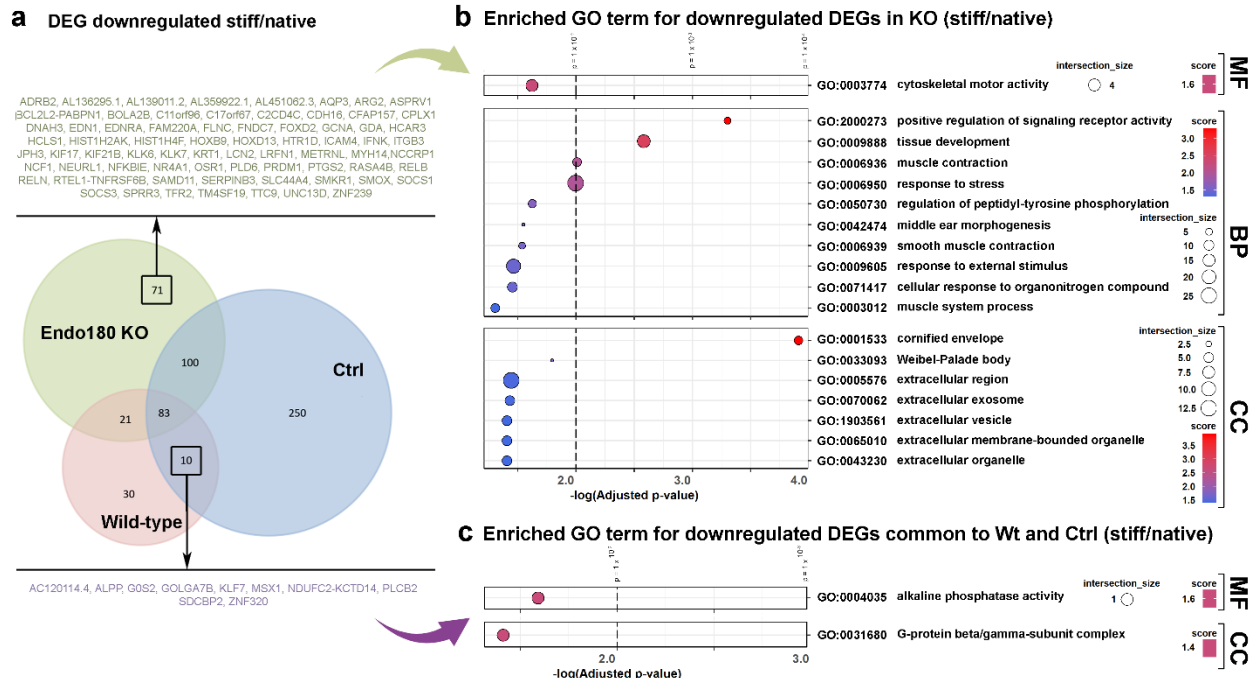
Alleles	Chr 17q23.2 position GRCh38	Chr 17q23.2 position GRCh37	Reference sequence ENSG00000011028	Mutated sequence
1	62664673	60742034	C	G
2	62664678	60742066	GTG	GCTG
3	62664705	60742039	ACCTGGGTACCATGCC GGCTATTCA	AAGAGTTGGTAGCTCTGATCACC TGGGTACCATGC,
				CCGGCTATTCAAGACCCTGCTGAA AGCTCTCGTGCAGCAGC

Supplementary Table 3. Mapping of Illumina RNA-seq reads in Ctrl-acini and Endo180-KO acini

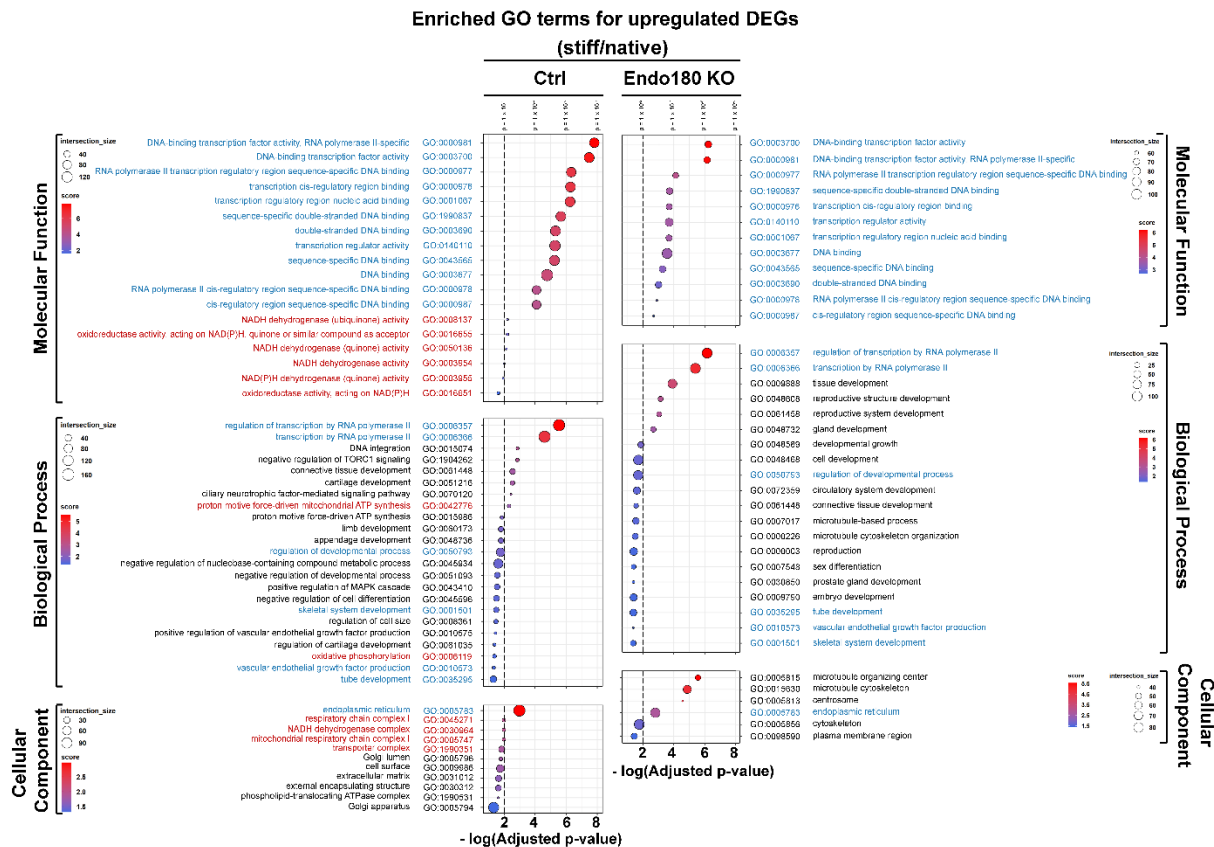
3D culture	Sample	Total reads	Total mapped reads (paired)*	Percent mapped
Ctrl native-BM	Ctrl n1	29268813	19901718	68.00
	Ctrl n2	19626732	11128753	56.70
	Ctrl n3	25732932	16092046	62.53
Ctrl stiff-BM	Ctrl s1	20059022	12533747	62.48
	Ctrl s2	26547795	15825029	59.61
	Ctrl s3	19109916	11304488	59.16
average % total mapped reads				61.42
KO native-BM	KO n1	21440281	14174531	66.11
	KO n2	24492619	16122925	65.83
	KO n3	26649588	17543642	65.83
KO stiff-BM	KO s1	22198268	15117163	68.10
	KO s2	21748999	12948340	59.54
	KO s3	21016733	14030576	66.76
average % total mapped reads				65.36
* reads mapped to annotated genes				
BM, basement membrane; Ctrl, control; KO, knockout; n, native; s, stiff				



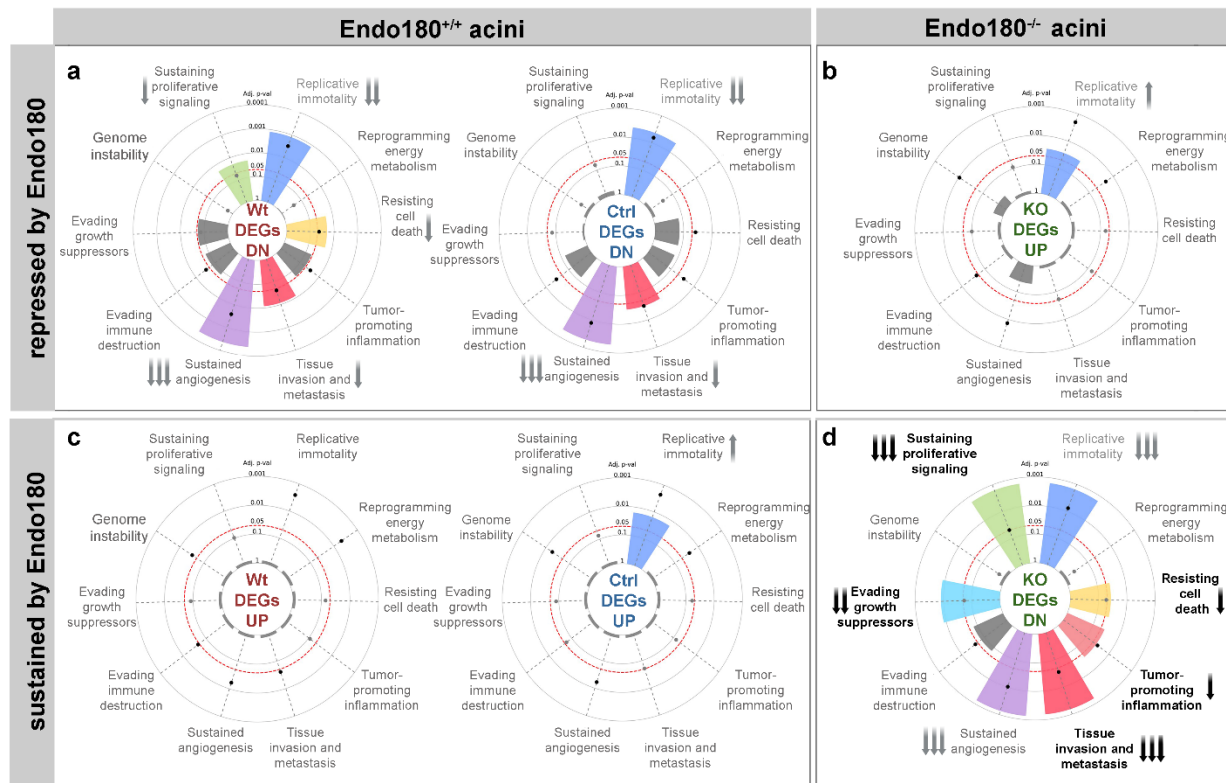
Supplementary figure 2. OXPHOS genes upregulated by basement membrane stiffness are common to wild-type and control prostate epithelia. a) Principal component analysis of DEGs in wild-type, Wt; control, Ctrl; and Endo180-knockout, KO; RWPE-1 acinar cultures grown in stiff versus native basement membrane (BM); expression rlog transformed values; three experimental repeats. **b)** Venn diagram shows number of exclusive and overlapping DEGs upregulated in Wt (pink), Ctrl (blue) or KO (green) acini in stiff versus native BM; (fold change ≥ 2 , FDR, p value < 0.05). DEGs only enriched in KO (green); or common to Wt and Ctrl acini (violet); are listed; note OXPHOS genes (bold text) are absent in KO. **c)** Gene ontology (GO) enrichments common to Wt and Ctrl acini grown in stiff versus native BM ranked in order of significance (-log₂ [adjusted p-values]); intersection size and scores, high: red; low: blue. GO terms common to Wt and Ctrl (red text) or only in Ctrl (black text). **d)** GO terms enriched only in KO; BP, biological process; CC, cellular component. Corresponding to Supplementary data 5 and 6.



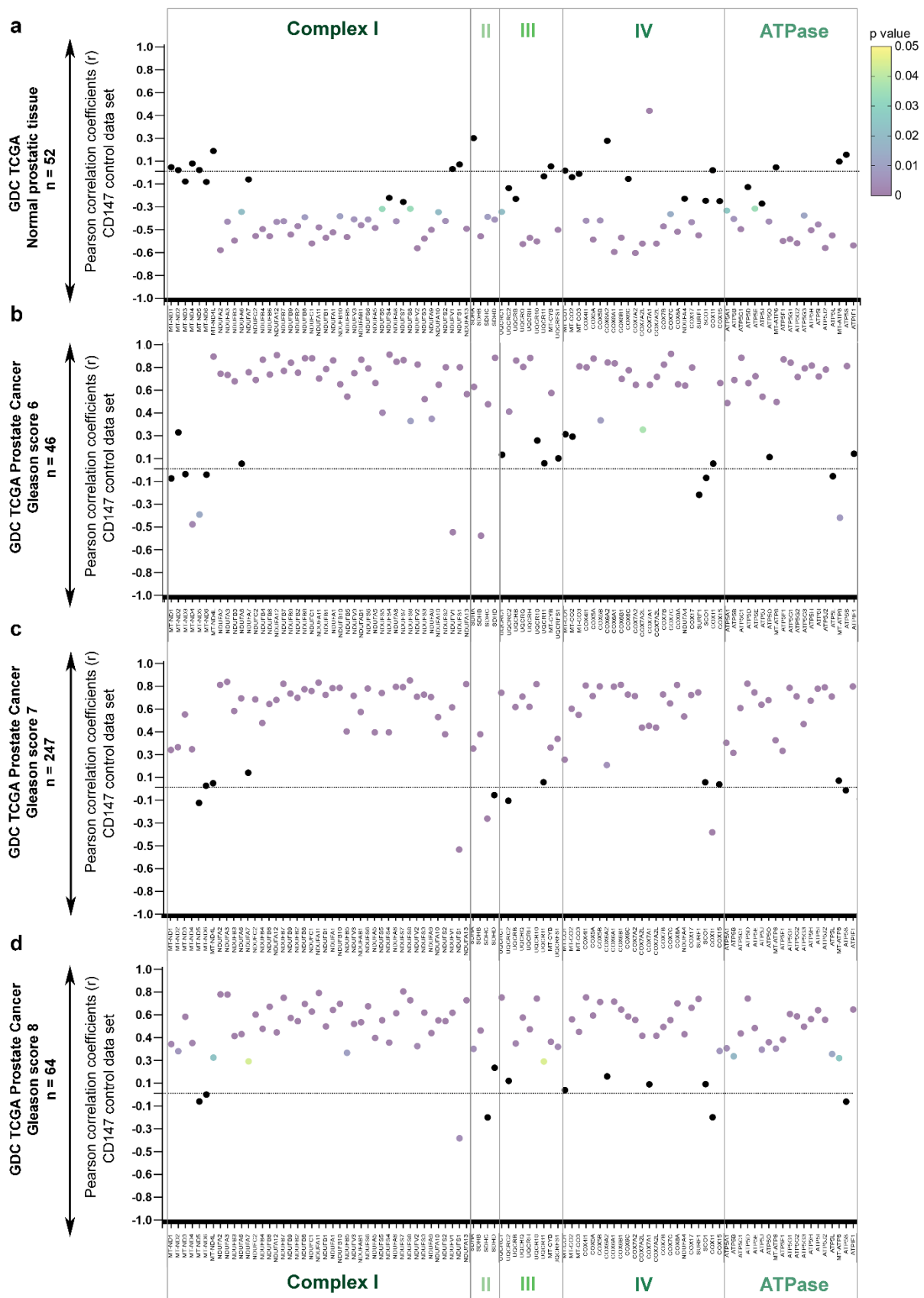
Supplementary figure 3. Downregulation of cytoskeletal motor activity, receptor-signaling, tissue development, exosomes and cornified envelope in Endo180-KO prostate epithelia. a) Venn diagram analysis showing overlapping or exclusively downregulated DEGs in Wt-acini (pink), Ctrl-acini (blue) and Endo180-KO-acini (green) in stiff-BM versus native-BM; fold change ≤ 2 , FDR p value < 0.05 ; numbers of DEGs within each sector of the Venn diagram are indicated; names of the DEGs upregulated exclusively in Endo180-KO acini (green) or common to Wt and Ctrl acini (violet) are indicated with OXPHOS genes highlighted in bold text. OXPHOS genes were not downregulated in Endo180-KO-acini. **b)** Gene ontology (GO) terms enriched with the 71 significantly downregulated DEGs exclusive to Endo180-KO-acini grown in stiff-BM versus native-BM; **c)** GO terms enriched with the 10 downregulated DEGs common to Wt-acini and Ctrl-acini grown in stiff-BM versus native-BM in order of their significance level (-log₂ [adjusted p-values]); intersection size and scores (red = high, blue = low) are shown. GO terms common to Wt-acini and Ctrl-acini (red text) or exclusive to Ctrl-acini (black text) are indicated. MF, molecular function; BP, biological process; CC, cellular component. Corresponding data in Supplementary data 5 and 6.



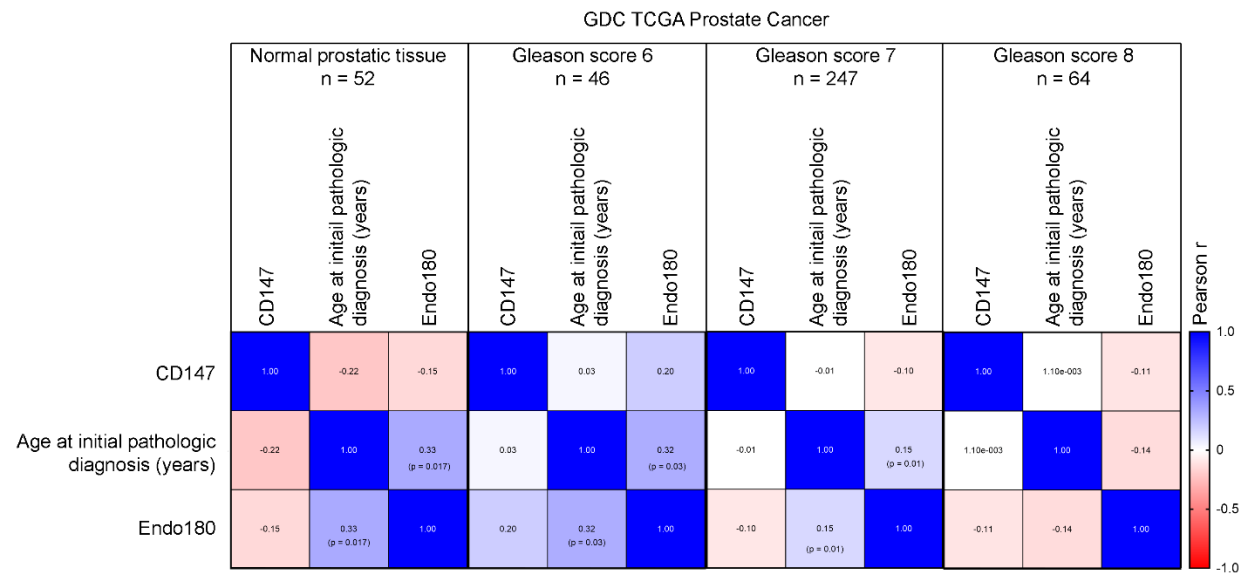
Supplementary figure 4. Gene ontology terms upregulated by basement membrane stiffness in control and Endo180-KO prostate epithelia. Gene ontology (GO) terms enriched with significantly upregulated DEGs (fold change ≥ 2 , FDR p value < 0.05) in control (Ctrl) (left) and Endo180-KO (right) prostate acinar epithelial cells (RWPE-1) grown in stiff-BM versus native-BM; GO terms are ranked in order of their significance level ($-\log_2$ [adjusted p-values]); intersection size and scores (red = high, blue = low) are shown. GO terms shared with Wt (in red text), common to Ctrl and Endo180-KO (in blue text) and exclusive to Ctrl or Endo180-KO (in black text). Corresponding data in Supplementary data 7 and 8.



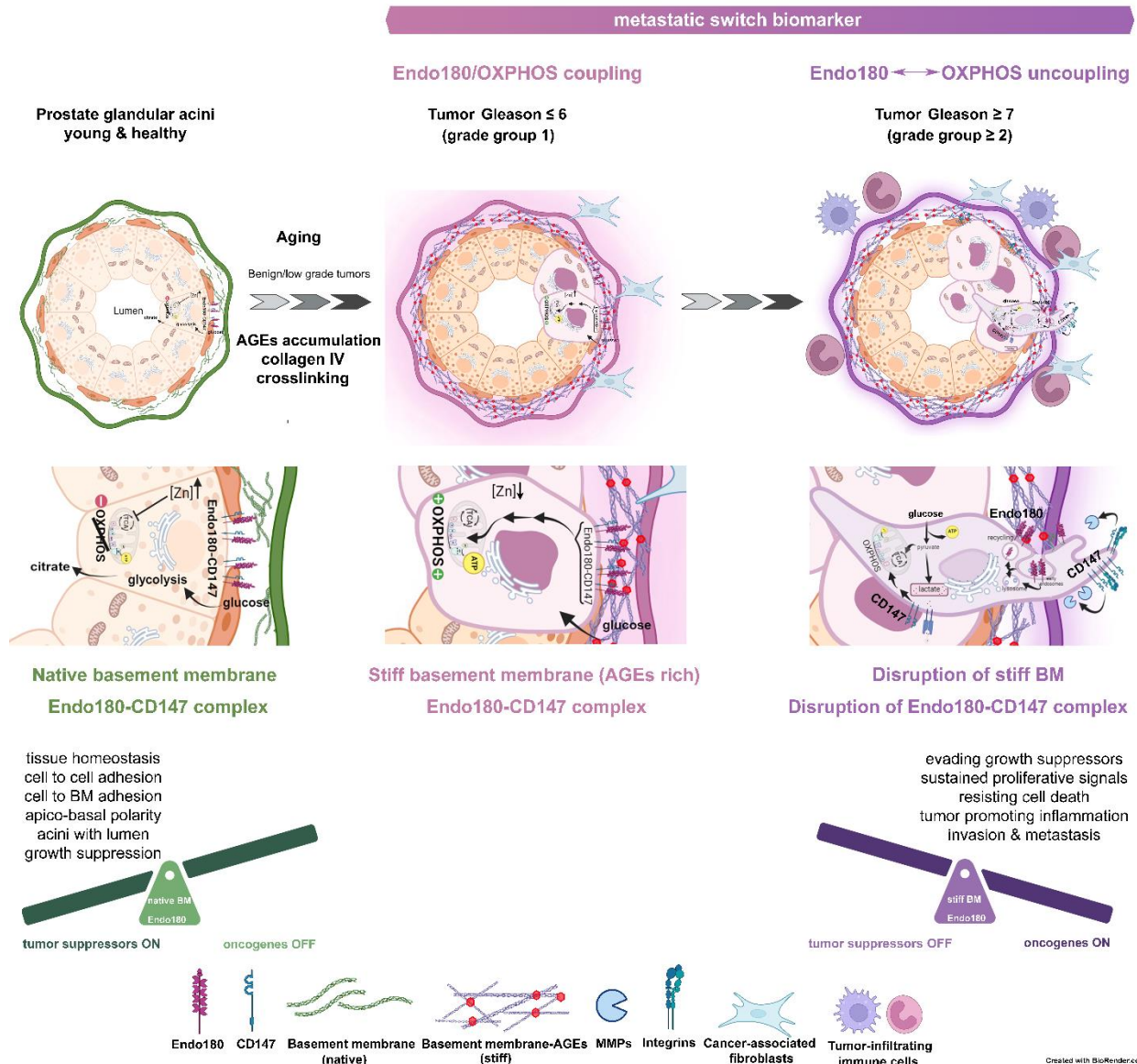
Supplementary figure 5. Endo180 and basement membrane stiffness cooperate to sustain the hallmarks of cancer in prostate epithelia. Integrated hallmarks of cancer gene consensus list ($n = 6763$) comparison to significantly **a, d**) downregulated (DN) or **b, c**) upregulated (UP) DEGs (fold change $\geq |2|$ FDR, p value < 0.05) in wild-type, Wt (red text, **a** and **c**), control, Ctrl (blue text, **a** and **c**) and Endo180 knockout, KO (green text, **b** and **d**), RWPE-1 acinar cultures grown in stiff-BM versus native-BM. Rose plot bars assigned a color indicate significant gene signature overlaps; concentric lines and arrows represent adjusted p -values of 0.05 (black line, one arrow), 0.01 (red line, two arrows) and 0.001 (black line, three arrows). Bold text and upward arrows indicate cancer hallmarks positively regulated (sustained); downward arrows indicate hallmarks negatively regulated (suppressed); in the presence (Wt, Ctrl) or absence (KO) of Endo180 in response to stiff-BM. Supplementary data **9** and **10** list the genes enriched for each cancer hallmark.



Supplementary figure 6. CD147 and OXPHOS genes remain positively correlated in Gleason score 6 and higher prostate cancer. Pearson correlation analysis of mitochondrial respiratory complexes I, II, III, IV and ATP synthase (WP111) genes and *BSG* (CD147) in the GDC-TCGA-PRAD dataset was performed on **a**) non-tumorigenic tumor-adjacent tissue (n = 52) and tumor tissue graded as **b**) Gleason 6, **c**) Gleason 7 (n=247) and **d**) Gleason 8 (n=64); expression unit: $[\log_2(\text{FPKM}-\text{uq}+1)]$; two-tailed Pearson correlation test ($\alpha = 0.05$) significant p values are coded on a yellow-to-purple scale; black dots = no significant correlation.



Supplementary data 7. Endo180 but not CD147 is positively correlated with age at initial prostate cancer diagnosis. Pearson correlation analysis of age at initial pathological diagnosis, *MRC2* (Endo180) and *BSG* (CD147) in the GDC-TCGA-PRAD dataset was performed on non-tumorigenic tumor-adjacent tissue (n = 52) and tumor tissue graded as Gleason 6, Gleason 7 (n=247) and Gleason 8 (n=64); significant r values are coded on a red-to-blue scale, negative correlation (red), positive correlation (blue); two-tailed Pearson correlation test ($\alpha = 0.05$).



Supplementary figure 8. Endo180 is an age-related time-bomb for metastatic prostate cancer. At basolateral surfaces of luminal epithelial cells Endo180-CD147 suppressor complex²² maintains tissue homeostasis in prostate glands with low biological age that have a low lifetime exposure to advanced glycation end products (AGEs). The high levels of zinc (Zn) in luminal epithelial cells of low biological age prostate glands inhibits mitochondrial aconitase switching off the citric acid cycle. This results in excessive levels of citrate secretion into the luminal space, promoting glucose transport and driving glycolysis for energy production. Prostate glands with high biological age have AGEs accumulation around acinar ducts that induce the Maillard reaction and formation of Amadori adducts, crosslinking collagen IV in the basement membrane¹⁰. Together with newly deposited collagen IV the basement membrane progressively thickens and stiffens. The increased rigidity of crosslinked collagen IV is sensed by Endo180, triggering a switch from glycolysis to mitochondrial oxidative phosphorylation (OXPHOS). This metabolic switching generates enough energy for sustained proliferation and early neoplasia. Endo180 also responds to biological aging and basement membrane stiffness by taking regulatory hold over hallmarks of cancer gene signatures for: (i) evading growth suppressors, (ii) sustaining proliferative signals, (iii) resisting cell death, (iv) tumor-promoting inflammation, and (v) invasion and metastasis. These events happen without any significant effect on genome instability or exposure to collagen I in the underlying stroma, revealing a new model for the evolution of age-related neoplasia. Exposure to HPV infection could contribute to replicative

immortality in this model by insertion of its E6 and E7 oncogenes into the epithelial cell genome. Endo180-CD147 suppressor complex is a time-bomb that can trigger the transition from clinical grade group 1 to grade group ≥ 2 tumors when it dissociates due to increased biological age. At this point Endo180 is internalized from the basolateral membrane into endosomes, activating the cytoskeletal motor, spatiotemporal F-actin cytoskeleton and microtubule remodeling, cell motility, chemotaxis and invasion. This coincides with CD147 release from the suppressor complex and its chaperoning of monocarboxylate transporter MCT4 that drives lactate secretion, OXPHOS and the Warburg effect as advanced prostate tumors progress.³⁰ Figure created with BioRender.com.

Supplementary table 4. Oligonucleotide sequences used in this study

Guide RNA	Gene	Exon 2	Sequence	Target gene sequence ID
	Endo180	E2b-sgRNA	CCGAAACCGGCTATTCAACCTGG	NG_033955.1
	Gene	Direction	Sequence	Reference sequence ID
Primers	beta actin	F	CACCCAGCACAAATGAAGATCA	NG_007992.1
		R	CTCGTCATACTCCTGCTTGC	
	GAPDH	F	TGTATCGTGGAGGGACTCA	NG_007073.2
		R	GCAGGGATGATGTTCTGGAG	
	MT-ND4L	F	CACCCACTCCCTCTTAGCCAAT	ENSG00000212907
		R	GGCCATATGTGTTGGAGATTGAGAC	
	MT-ND2	F	CTCCAGCACCACGACCCCTAC	ENSG00000198763
		R	CAAAAAGCCGGTTAGCGGGG	
	MT-ND1	F	GACGCACTCTCCCCTGAACT	ENSG00000198888
		R	CGTAGCGGAATCGGGGGTAT	
	MT-CO3	F	CTCCGGCCTAGCCATGTGAT	ENSG00000198938
		R	TTCTCGTGTACATCGGCC	
	MT-CO1	F	CGCCCCTTCGCTGTGATCC	ENSG00000198804
		R	GGTGTGAGGTTGCGGTCTG	
	MT-ATP8	F	TACCACCTACCTCCCTCACCA	ENSG00000228253
		R	GGGGCAATGAATGAAGCGAAC	
	rRNA 18s	F	CGCGGTTCTATTTGTTGGT	NR_145820.1
		R	AGTCGGCATCGTTATGGTC	
	Endo180 qPCR	F	GGATGAGATGGAGAACGTGTTG	NG_033955.1
		R	CAGTTGGAGTAGTCACAGCT	
	Endo180	F	TTTGAGGGTGGTACAGAGGAC	
		R	AATCTGTCCTCATGGCTCC	
	MIGA2	F	GTGGACAAGGGACTTCAGG	NM_001329990.2
		R	CCACAACAACCCCTCTCTC	
	L1CAM	F	CCATCTCACTCAGCCTCACG	NM_001278116.2
		R	GGCCTTGCACAGAAGGTAGG	